Journal of
Nanoscience and Nanotechnology
Vol. 13, 7950–7954, 2013

RESEARCH ARTICLE

Free-Standing Nitrogen-Doped Reduced Graphene Oxide Anode for Lithium-Ion Batteries

Hyun Ho Park, Youngeun Choi, Bona Kim, Young Soo Yun, and Hyoung-Joon Jin*

Department of Polymer Science and Engineering, Inha University, Incheon 402-751, Korea

Graphenes have been considered suitable candidate materials for electrodes of energy storage devices such as lithium-ion batteries (LIBs) because of their outstanding mechanical, thermal and electrical properties. However, there are problems when using these carbon materials for electrodes because of their low electrochemical performance. In this work, to improve the electrochemical performances of graphenes, free-standing nitrogen-doped reduced graphene oxides (FNRGOs) were prepared as an anode for LIBs using a facile vacuum filtration method and thermal annealing at different temperatures. X-ray diffraction and X-ray photoelectron spectroscopy were employed to characterize the prepared samples, and then their electrochemical performance was investigated by galvanostatic charge/discharge (GCD) tests. GCD tests revealed that FNRGO prepared from thermal annealing at 500 °C exhibited good initial reversible capacity (502 mA h/g at 50 mA/g (0.14 C)) and enhanced cycle stability (capacity retention of 90.5% after 50th cycles at 100 mA/g (0.27 C), which demonstrated that FNRGOs were suitable candidates as anodes for LIBs.

Keywords: Nitrogen, Graphene, Free-Standing Electrode, Anode, Li-Ion Batteries.

1. INTRODUCTION

Lithium-ion batteries (LIBs), one of the most promising rechargeable batteries, have attracted significant interest for use in electric vehicles and portable devices, because of their high voltage, low self-discharge, long cycling life, low toxicity and high reliability.[1] These days, there is much demand for LIBs with high performance for use in portable, entertainment computing and telecommunication equipment.[2–4] LIB cells are basically composed of four main components: an anode, cathode, electrolyte and separator. The anode supplies electrons to the external circuit when oxidized during discharge, and the electrochemical performance of LIBs mainly depends on the physical/chemical properties of the anode material. In general, graphite is the most commonly used owing to its appropriate structure for ionic, atomic and molecular species to diffuse between the graphite layers and to form intercalation compounds as well as stable specific capacity and good cycle stability.[5] But, with graphitic carbon anode materials for LIBs, the maximum theoretical lithium storage capacity of LIBs is 372 mA h/g, because lithium forms LiC_6 intercalation compounds, which limit lithium ion storage sites. Recently, many research groups have focused on developing various carbonaceous nanomaterials with high lithium storage properties.

Graphene has gained much attention for applications in energy devices such as electrochemical capacitors and LIBs because of its superior electrical properties, excellent thermal properties, chemical stability and a broad window potential.[6–11] However, in graphene-based materials as anode for LIBs, there are limits and restrictions due to low initial reversible capacity and Coulombic efficiency. Heteroatom-doping has been demonstrated as an effective method to improve the electrochemical performance of graphene. Graphene-based material doping with nitrogen has especially attracted much interest because nitrogen-doping can change the band structure of graphene and lead to *n*-type semiconductor transition.[12–14] For nitrogen-doped graphene, the various nitrogen atomic states such as pyridinic-, pyrrolic- and graphic nitrogen atoms could significantly improve electrochemical performance, offer more active sites on the graphene nanostructure by making defect sites from doping with nitrogen, and enhance the lithium-intercalation between graphene nanostructured layers (including defect sites) and lithium-ions. This may be helpful for the electrochemical performance of LIB anodes by the improvement of lithium-ion diffusion and transfer with respect to the kinetics.

"Free-standing" carbon-based nanostructures as electrodes for energy devices have received incredible attention for fundamental and practical applications.[15, 16] Free-standing electrodes, without any polymer binder or conducting materials, could significantly improve the

*Author to whom correspondence should be addressed.

 1533-4880/2013/13/7950/005 doi:10.1166/jnn.2013.8108

specific capacity per weight and reduce manufacturing costs compared to electrodes made with binder and conducting materials.[17–19]

In this study, we prepared free-standing nitrogen-doped reduced graphene oxides (FNRGOs) based on graphene oxide (GO) and melamine by using vacuum filtration and thermal annealing, and their electrochemical performance was subsequently investigated.

2. EXPERIMENTAL DETAILS

2.1. Materials

GO was prepared from natural graphite flake (Sigma-Aldrich, Product Number 332461) by the Hummers method.[20] Melamine monomer (99%) was obtained from Aldrich.

2.2. Preparation of Free-Standing GO/Melamine

Free-standing GO/melamine was fabricated by vacuum filtration. In a typical procedure, the GO powder obtained from the Hummers method was diluted to the concentration of 0.5 mg/ml using deionized water, and then GO solution was well dispersed using ultrasound. Then, the melamine monomer was added into the GO solution with vigorous stirring until it was completely dissolved. Free-standing GO/melamine was made by vacuum filtration of the resulting GO and melamine solution using a Whatman Anodisc™ membrane filter (0.2 μm pore size, 47 mm in diameter), followed by drying in air and peeling from the filter.

2.3. Preparation of Free-Standing Nitrogen-Doped Reduced GOs (FNRGOs)

The free-standing GO/melamines were annealed in a horizontal furnace under a pure nitrogen gas atmosphere at a heating rate of 10 °C/min to final temperatures of 500, 600, and 800 °C, and then maintained at these temperatures for 2 h. To confirm the effects of nitrogen on electrochemical performance, free-standing reduced GOs (FRGOs) were prepared in the same method without melamine monomer.

2.4. Characterization

X-ray diffraction (XRD, Rigaku, DMAX-2500, Japan) was used to characterize the samples through a diffractometer with reflection geometry and CuKα radiation (wavelength $\lambda = 0.154$ nm) operated at 40 kV and 100 mA. The data were collected within the range of scattering angles (2θ) from 5° to 60° with a scanning rate of 1 °/min. The chemical state and surface composition of the samples were measured with X-ray photoelectron spectroscopy (XPS, AXIS-HIS, Kratos Analytical, Japan). XPS spectra were recorded using a dual-chromatic MgKα X-ray source at 1500 eV. High-resolution XPS spectra were recorded at 0.05 eV steps with pass energy of 20 eV.

2.5. Electrochemical Measurements

The electrochemical performance of the samples was characterized by a half-cell with a Wonatec automatic battery cycler in a CR2016-type coin cell. The working electrodes were directly fabricated without polymer binders or other conducting additives, and punched into round shapes. A solution of 1 M $LiPF_6$ (Aldrich 99.99%) in ethylene carbonate/dimethyl carbonate/diethyl carbonate (1:2:1 volume ratio) and lithium metal foil were used as the electrolyte and the reference electrode, respectively. The coin cells were assembled in an argon-filled glovebox, and subsequently measured in the potential range of 0.01 to 3 V versus Li/Li^+ at various current densities between 50 to 1000 mA/g (between 0.3 to 2.7 C) through galvanostatic charge/discharge (GCD) tests.

3. RESULTS AND DISCUSSION

Figure 1 shows the SEM image of cross-section structure for FNRGO500. FNRGO500 revealed well-packed graphene layers through almost the entire cross-section.

Figure 2(A) shows the XRD patterns of free-standing GO and free-standing GO/Melamine. For free-standing GO, the diffraction peak was mainly revealed 11.4° at 2θ (interlayer spacing: 0.78 nm), which is attributed to the (002) crystalline plane of GO. In the case of free-standing GO/melamine, its diffraction peak shifted to a lower scattering angle (10.2° at 2θ) than that of free-standing GO, which is deduced that the distance between the graphene layers was increased by adding melamine molecules (interlayer spacing: 0.87 nm). It was confirmed that the melamine molecules were absorbed on the basal plane and edge of GO by forming hydrogen bonding between hydroxyl and carboxyl groups of GO and amine groups of melamine. As shown in Figure 2(B), after thermal annealing of free-standing GO at various temperatures, FNRGO500, FNRGO600 and FNRGO800 exhibited

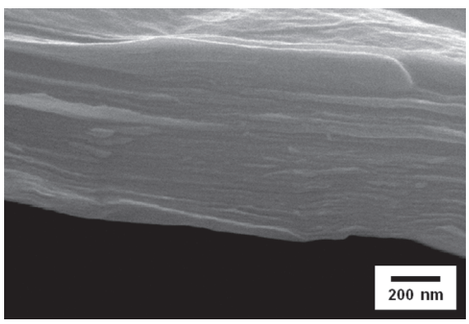

Fig. 1. SEM image of FNRGO500.

RESEARCH ARTICLE

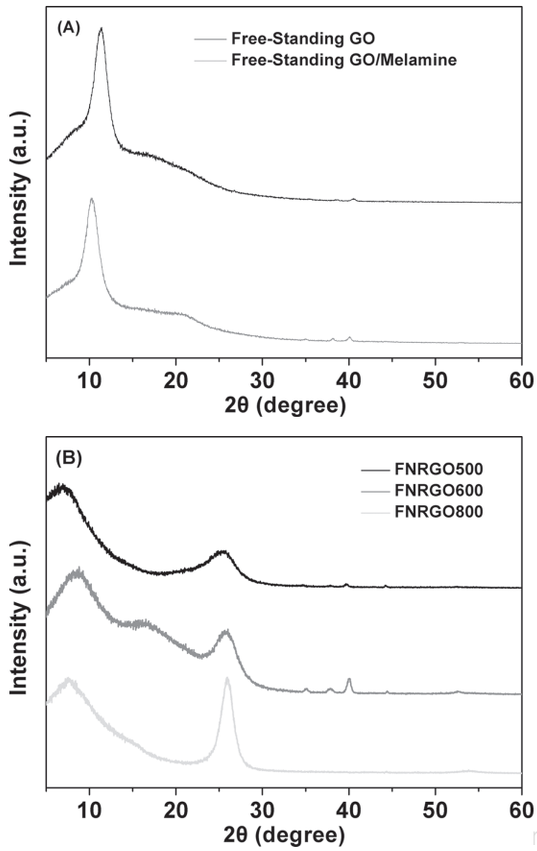

Fig. 2. XRD patterns of (A) free-standing GO and free-standing GO/Melamine, and (B) FNRGO500, FNRGO600 and FNRGO800.

similar main peaks at about 7–8° (interlayer spacing: 1.1–1.2 nm) and 25–26° (interlayer spacing: 0.34–0.36 nm) at 2θ. There are two main reasons: the distance between graphene layers was increased because of releasing NH_3 and H_2O gas (0.87 to 1.1 nm), while the graphite (002) plane was restored through the reduction of GO, which indicated the recovery of the π–π conjugated system. It means heterogeneity of FNRGOs not physical mixing.

To confirm the nitrogen-doping of the free-standing GO, XPS studies were conducted. Figure 3 shows the survey scan spectra of free-standing GO, FNRGO500, FNRGO600 and FNRGO800 from XPS. For free-standing GO (Fig. 3(A)), there were two peaks for core levels of C1s and O1s at 284 and 532 eV, respectively, with no impurities. After thermal annealing for free-standing GO/Melamine, the survey data of FNRGOs showed the presence of N1s core level at 399 eV, as well as peaks of C1s and O1s, which demonstrated that the free-standing reduced GO was doped with nitrogen atoms. For quantitative analysis, the elemental composition of the surface in the form of atomic content obtained from XPS data of the samples is presented in Table I. According to the XPS data, the contents of the nitrogen and oxygen atoms were decreased, and the contents of the carbon atoms were increased as the annealing temperature

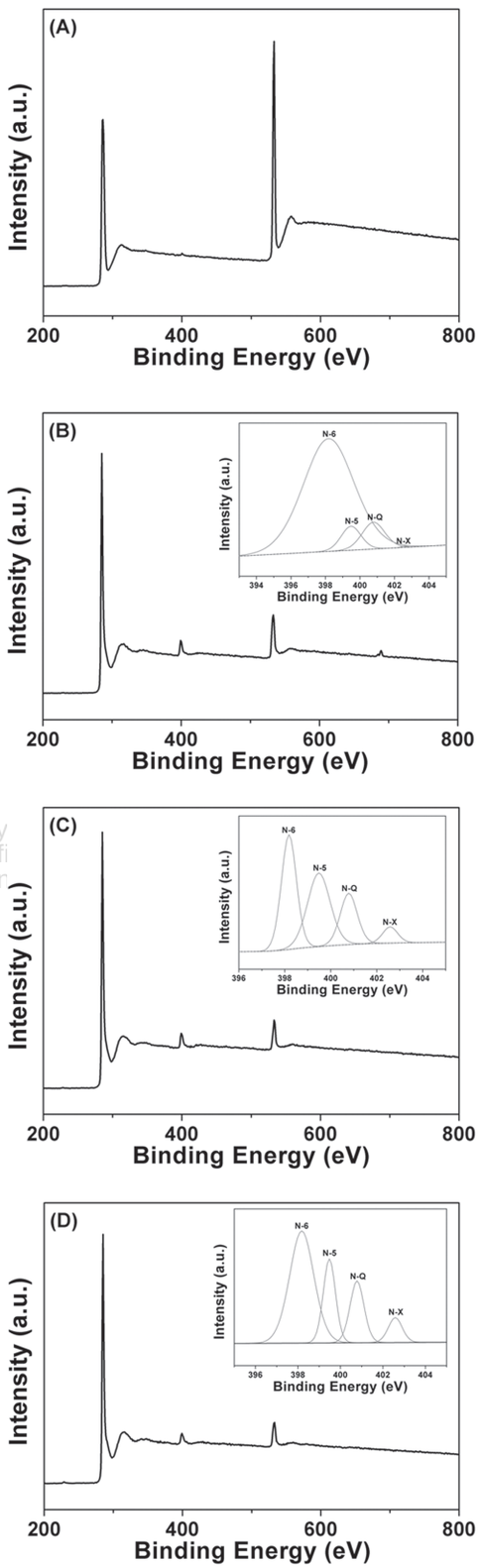

Fig. 3. Survey data from XPS spectra of (A) Free-Standing GO, (B) FNRGO500, (C) FNRGO600 and (D) FNRGO800. The inset shows the XPS spectra of N1s of (B) FNRGO500, (C) FNRGO600 and (D) FNRGO800.

Table I. Elemental composition by XPS (At%).

	C	N	O
Free-standing GO	72.9		27.2
FNRGO500	84.8	6.5	8.7
FNRGO600	88.7	5.3	6.0
FNRGO800	90.0	4.4	5.6

increased. For nitrogen atoms, FNRGOs had a considerable amount of nitrogen because of the thermal annealing at relatively low temperature. It has been reported in many studies that nitrogen atoms play an important role in the anode of LIBs due to strong interaction between nitrogen atoms and lithium ions. Thus, it is expected that the incorporation of nitrogen atoms into free-standing reduced GO could influence the electrochemical performance.

The charge and discharge curves of FNRGO500 are shown in Figure 4(A). The existence of the plateau region at about 0.6 V indicated the formation of a solid-electrolyte-interphase film.[21] The capacity of the potential region lower than 0.5 is due to Li^+ intercalation into the graphene layers during charge process. The absence of a potential plateau suggests electrochemically and geometrically nonequivalent Li^+ sites.[22] At current density of 50 mA/g, FNRGO500 had 791 and 397 mA h/g at 1st and 2nd charge process, respectively, and 502 and 377 mA h/g at 1st and 2nd discharge process, respectively. To prove the effects of nitrogen on the LIB anodes, the rate performance obtained from the GCD curves of FNRGO500 and FRGO500 are indicated in Figure 4(B). Under low current density of 50 mA/g (0.14 C) and high current density of 1000 mA/g (2.7 C), FNRGO500 exhibited initial reversible capacities of 502 and 88 mA h/g, respectively, while FRGO500 exhibited initial reversible capacities of 423 and 54 mA h/g, respectively. In addition, the capacities of FNRGO500 were higher than those of FRGO500 between 50 and 1000 mA/g (0.14 to 2.7 C). This means that nitrogen doping was effective compared to the anode without nitrogen doping. In the case of FNRGO500, strong interaction between carbon layer atoms and lithium ions might be due to the higher electronegativity and smaller diameter of nitrogen atoms compared to carbon atoms, and thus more lithium ion may be intercalated.[23] In addition, because of defects produced by nitrogen-doping and the strong bond between nitrogen atoms and lithium ions, nitrogen-doping could enhance the rate performance of the reduced GO.

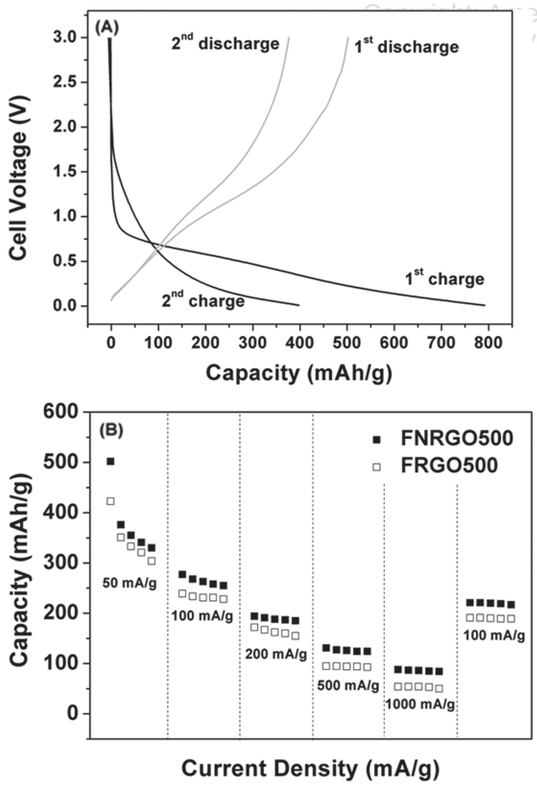

Fig. 4. (A) Charge/discharge curves of FNRGO500 and (B) rate performance of FNRGO500 and FRGO500.

Figure 5 shows the rate performance obtained from the GCD curves of FNRGO500, FNRGO600 and FNRGO800 to confirm the effects of nitrogen contents for the LIB anodes. For FNRGO500, which included higher nitrogen contents (6.5 At%) than other samples (FNRGO600: 5.3 At%, FNRGO800: 4.4 At%), its reversible capacities at all corresponding current densities were higher than those of FNRGO600 and FNRGO800, which indicated that higher nitrogen contents resulted in higher initial capacities. Also, in many researches, it was demonstrated that chemical states of nitrogen as well as nitrogen-content are very important for the capacitive behaviors. As shown in Table II and the inset of Figure 3, FNRGO500 had large amount of pyridinic- and pyrrolic-nitrogen than those FNRGO600 and FNRGO800. These five valence electrons atoms play role in the additional charge to the π-bond in graphene layers, which enhances the basicity of carbon and the electrical conductivity of nitrogen-doped carbon.[24]

Figure 6 shows the discharge capacities versus the cycle number. For FNRGO500, it can be observed that its cycle

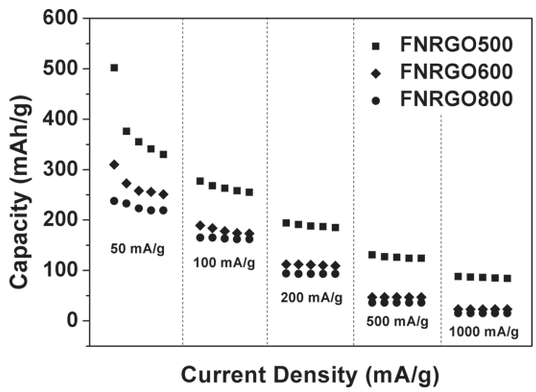

Fig. 5. Rate performance of FNRGO500, FNRGO600 and FNRGO800.

Table II. Relative surface concentrations of nitrogen species obtained by fitting the N1s core level XPS (At%).

	N-6 (%)	N-5 (%)	N-Q (%)	N-X (%)
FNRGO500	84.0	7.0	8.9	0.1
FNRGO600	38.3	36.9	19.3	5.5
FNRGO800	55.0	20.6	17.4	7.0

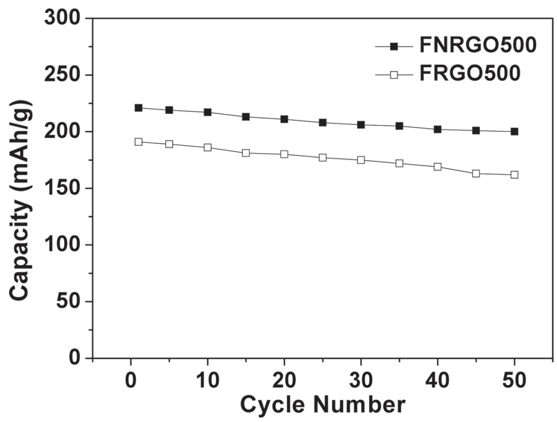

Fig. 6. Cycle performance of FNGRO500 and FRGO500 at current density of 100 mA/g.

stability was considerably enhanced at the current density of 100 mA/g (0.27 C). After 50 cycles, FNRGO500 had a capacity retention of 90.5% (from 221 mA h/g at 1st discharge to 200 mA h/g at 50th discharge), while FRGO500 had a capacity retention of 85% (from 191 mA h/g at 1st discharge to 162 mA h/g at 50th discharge). These results demonstrated the importance of the nitrogen atoms in enhancing the cycle stability of LIB anodes. Nitrogen-doped carbon materials may be useful for reducing the catalysis reaction, thus enhancing the cycle stability of the FNRGO500 during cycling steps.

4. CONCLUSIONS

We successfully prepared free-standing reduced graphene oxide by doping with nitrogen via vacuum filtration and thermal annealing. We were able to confirm that free-standing GO was doped with nitrogen atoms using thermal annealing for melamine by XPS data. The GCD results showed that the electrochemical performance of FNRGO500s was better than that of FRGO500 because of the effects of nitrogen atoms, such as strong bond between nitrogen atoms and lithium ions. FNRGO500, FNRGO600 and FNRGO800, which were annealed at different temperatures, had different nitrogen contents of 6.5, 5.3 and 4.4 At%, respectively, and FNRGO500 had large amount of pyridinic- and pyrrolic-nitrogen than those FNRGO600 and FNRGO800, which play roles for improving capacities. In addition, FNRGO500 showed superior electrochemical performance compared to FNRGO600 and FNRGO800.

Acknowledgments: This work was supported by the National Research Foundation of Korea Grant funded by the Korean Government (MEST) (NRF-2010-C1AAA001-0029018).

References and Notes

1. C. Liu, F. Li, L.-P. Ma, and H.-M. Cheng, *Adv. Mater.* 22, E28 (**2010**).
2. J.-M. Tarascon and M. Armand, *Nature* 414, 359 (**2001**).
3. M. Armand and J.-M. Tarascon, *Nature* 451, 652 (**2008**).
4. K. Kang, Y. S. Meng, J. Breger, C. P. Grey, and G. Ceder, *Science* 311, 977 (**2006**).
5. N. A. Kaskhedikar and J. Maier, *Adv. Mater.* 21, 2664 (**2009**).
6. A. K. Geim and K. S. Novoselov, *Nat. Mater.* 6, 183 (**2007**).
7. M. Liang and L. Zhi, *J. Mater. Chem.* 19, 5871 (**2009**).
8. E. Yoo, J. Kim, E. Hosono, H.-S. Zhou, T. Kudo, and I. Honma, *Nano Lett.* 8, 2277 (**2008**).
9. Z.-L. Ding, J. Jiang, H.-B. Shu, X.-S. Chen, and W. Lu, *J. Nanosci. Nanotechnol.* 11, 10778 (**2011**).
10. J. H. Kim, J. M. Jung, J. Y. Kwak, S.-S. Hong, Y.-S. Gal, and K. T. Lim, *J. Nanosci. Nanotechnol.* 12, 4294 (**2012**).
11. J. Yuan and K. M. Liew, *J. Nanosci. Nanotechnol.* 12, 2617 (**2012**).
12. H. Wang, C. Zhang, Z. Liu, L. Wang, P. Han, H. Xu, K. Zhang, S. Dong, J. Yao, and G. Cui, *J. Mater. Chem.* 21, 5430 (**2011**).
13. X. Li, D. Geng, Y. Zhang, X. Meng, R. Li, and X. Sun, *Electrochem. Commun.* 13, 822 (**2011**).
14. D. Geng, S. Yang, Y. Zhang, J. Yang, J. Liu, R. Li, T.-K. Sham, X. Sun, S. Ye, and S. Knights, *Appl. Surf. Sci.* 257, 9193 (**2011**).
15. D. A. Dikin, S. Stankovich, E. J. Zimney, R. D. Piner, G. H. B. Dommett, G. Evmenenko, S. T. Nguyen, and R. S. Ruoff, *Nature* 448, 457 (**2007**).
16. O. C. Compton, D. A. Dikin, K. W. Putz, L. C. Brinson, and S. T. Nguyen, *Adv. Mater.* 22, 892 (**2010**).
17. S. H. Ng, J. Wang, Z. P. Guo, J. Chen, G. X. Wang, and H. K. Liu, *Electrochim. Acta* 51, 23 (**2005**).
18. A. Abouimrane, O. C. Compton, K. Amine, and S. T. Nguyen, *J. Phys. Chem. C* 114, 12800 (**2010**).
19. A. L. M. Reddy, A. Srivastava, S. R. Gowda, H. Gullapalli, M. Dubey, and P. M. Ajayan, *ACS Nano* 4, 6337 (**2010**).
20. W. S. Hummers and R. E. Offeman, *J. Am. Chem. Soc.* 80, 1339 (**1958**).
21. P. Guo, H. H. Song, and X. H. Chen, *Electrochem. Commun.* 11, 1320 (**2009**).
22. Z. H. Yang and H. Q. Wu, *Mater. Lett.* 50, 108 (**2001**).
23. Y. P. Wu, S. B. Fang, and Y. Y. Jiang, *Solid State Ionics* 120, 117 (**1999**).
24. Y. Shao, X. Wang, M. Engelhard, C. Wang, S. Dai, J. Liu, Z. Yang, and Y. Lin, *J. Power Sources* 195, 4375 (**2010**).

Received: 15 May 2012. Accepted: 20 December 2012.